

Tuned Red NIR phosphorescence of polyurethane hybrid composites embedding metallic nanoclusters for oxygen sensing.

M. Amela-Cortes,^{a,b*} S. Paofai,^a S. Cordier,^a H. Folliot^c and Y. Molard^{a*}

Electronic supplementary informations

Experimental details:	2
Synthesis:	2
Table S1. Thermal behaviour of doped PUxH and PUxF samples	3
Fig. S1 TGA thermograms obtained at 10 K min ⁻¹ heating rate for a) Cs ₂ Mo ₆ I ₈ (OCOC ₂ F ₅) ₆ b) PUxF samples and c) PUxH samples, black line: x = 0; red line: x = 1; blue line: x = 10; green line: x = 20; magenta line: x = 50.	3
Fig. S2 DSC Thermograms of PUxH samples with a) PU0H, b) PU1H, c) PU10H and d) PU20H; A: first heating, B) first cooling, C) second heating, D) second cooling.	4
Fig. S3 DSC thermograms obtained on heating at 10 K min ⁻¹ for PUxF samples.....	4
Fig. S4 DSC thermograms obtained on cooling at 10 K min ⁻¹ for PUxF samples	5
Fig. S5 Normalized luminescence spectra obtained for PUxF (left) and PUxH (right) samples under irradiation at 360 nm.....	6
Fig. S6 Evolution of the absolute quantum yield of a PU50F sample placed within the integrating sphere upon constant N ₂ gas flow (P= 0.4 mbar).....	6
Fig. S7 Evolution of the quantum yield values upon air/N ₂ atmosphere cycling, right: pictures taken under irradiation (integration time:100ms) of PUxF samples	6
Table S2. Photophysical parameters of PUxF (x=n 1, 10, 50) under air and N ₂ gas stream	7
Figure S8 Phosphorescence decay profiles (in black) and calculated fit (in red) for PU1F in air (left) and with a N ₂ stream (right)	7
Figure S9 Phosphorescence decay profiles (in black) and calculated fit (in red) for PU10F in air (left) and with a N ₂ stream (right).....	7
Figure S10 Phosphorescence decay profiles (in black) and calculated fit (in red) for PU50F in air (left) and with a N ₂ stream (right)	7

Experimental details:

Starting materials were purchased from Aldrich and used without further purification. NMR spectra were recorded on a Bruker 400P. All signals were referenced to the methyl signals of TMS at $\delta = 0$ ppm. UV-Vis absorption measurements were performed on a Varian Cary 5000 UV-Vis-NIR spectrophotometer. Luminescence spectra were recorded with an ocean optic QE6500 photodetector mounted on an optical microscope, equipped with a Nikon Intensilight irradiation source. In order to take into account the nonlinear sensitivity of the set up, it was calibrated with an Ocean Optics HL-2000-CAL Calibrated Tungsten Halogen Light Source. Optical filters were used to select the excitation wavelength with a bandwidth: 330-380 nm. Elemental Analysis were performed at the CRMPO with a Microanalyser Flash EA1112 CHNS/O Thermo Electron. Energy dispersive spectroscopy (EDS) was performed at CMEBA on a JEOL 6400 scanning electron microscope equipped with a XEDS Oxford field spectrometer. DSC measurements were realized at $10 \text{ K}\cdot\text{min}^{-1}$ with a DSC 200 F3 Maia NETSCH apparatus. Thermogravimetric analysis was realized at $10 \text{ K}\cdot\text{min}^{-1}$ on a TGA/DT Perkin Pyris Diamond.

The luminescence quantum yields in the solid state were measured with a C9920-03 Hamamatsu system equipped with a 150 W xenon lamp, a monochromator, a Spectralon integrating sphere connected to N_2 gas line and a PMA-12 photomultiplier. The atmosphere of the integrating sphere was saturated with N_2 gas by passing a continuous 0.4 mbar flow.

Lifetime measurements were performed using APD110A Thorlabs Si avalanche photodiode and MPL-F-355 CN1 355 Q-switched laser with $\sim 7\text{ns}$ - $1\mu\text{J}$ pulses and 6kHz repetition rate. Traces were recorded using Lecroy 12 bit HDO4022 200MHz oscilloscope with 256 averaging. The luminescence was collected at normal incidence with numerical aperture of ~ 0.16 using parabolic mirrors, spectrally filtered with a high pass 500nm filter and focused on the detector using another parabolic mirror.

Synthesis:

Catp-Br: 3-dimethylaminopropanol (1.55 g, 15 mmol) and 11-bromoundecane (3.06 g, 13 mmol) were mixed and refluxed at 80°C for 30 min. The reaction mixture was cooled to room temperature and 1:3 (v/v) propanol : methanol was poured into the flask. After 12 h of reaction at 80°C , the solvents were evaporated and the product was purified by washing twice with diethyl ether. Yield 82%.

CatP-Br: $^1\text{H-NMR}$ (400 MHz, CDCl_3): δ (ppm) = 4.52(s, 1H, OH), 3.75 (m, 4H, $\text{CH}_2\text{-OH} + \text{CH}_2\text{-N}$), 3.42 (m, 2H, $\text{CH}_2\text{-N}$), 3.31(s, 6H, $-\text{CH}_3\text{-N}$), 2.18 (m, 2H, $\text{CH}_2\text{CH}_2\text{N}$), 1.78 (m, 2H, $\text{CH}_2\text{CH}_2\text{N}$), 1.35-1.26 (m, 16H, $-\text{CH}_2-$), 0.88 (t, 3H, $-\text{CH}_3$). $^{13}\text{C-NMR}$ (400 MHz, CD_2Cl_2): 63.92 (C-O), 62.01 ($\text{CH}_2\text{-N}$), 57.96 ($\text{CH}_2\text{-N}$), 50.55 ($\text{CH}_3\text{-N}$), 31.76 ($-\text{CH}_2-$), 26.23 ($-\text{CH}_2-$), 25.93 ($-\text{CH}_2-$), 13.50 ($-\text{CH}_3$). ESI-MS (m/z): 258.28. Elemental analysis for $\text{C}_{17}\text{H}_{38}\text{NOBr}\cdot 0.5\text{H}_2\text{O}$: calc (%): C 55.32, H 10.74, N 4.03. Found: C 55.84, H 1.61, N 4.04.

Compound 2 (Catp) $_2$ [$\text{Mo}_6\text{I}_8(\text{OCOC}_2\text{F}_5)_6$]

CatP-Br (1.2 g, 35 mmol) was dissolved in acetone. A solution in acetone of fluorinated cluster (0.5 g, 17.6 mmol) was added and the mixture stirred for 1h. The acetone was removed and the residue was solubilised in dichloromethane and the solution filtered through Celite®. The solvent was evaporated to yield a dark orange oil. Yield = 92%

$^1\text{H-NMR}$ (400 MHz, CDCl_3): δ (ppm) = 3.91 (s, 2H, OH), 3.57 (m, 4H, $\text{CH}_2\text{-OH}$), 3.53 (m, 4H, $\text{CH}_2\text{-N}$), 3.42 (m, 4H, $\text{CH}_2\text{-N}$), 3.20(s, 12H, $-\text{CH}_3\text{-N}$), 2.08-1.70 (m, 8H, $-\text{CH}_2-$), 1.28-1.15 (m, 32H, $-\text{CH}_2-$), 0.74 (t, 6H, $-\text{CH}_3$). $^{19}\text{F-NMR}$: δ (ppm) = -82.97 (3F), -120.62 (2F). Elemental analysis for $\text{C}_{50}\text{H}_{74}\text{N}_2\text{F}_3\text{O}_18\text{Mo}_6$, $20\text{CH}_2\text{Cl}_2$: calc (%): C 17.56, H 2.40, N 0.59. Found: C 17.55, H 2.02, N 0.60.

Synthesis of polyurethane nanocomposites

A mixture of 1,6-butanediol and compound 2 (from 1 to 50 wt.%) was heated to 50°C to melt. To that the hexamethylenediisocyanate (HDI) was added under argon and the reaction was left for 4h under Ar. The polymer was purified by washing with methanol twice and filtering off. The product was dried under vacuum to yield an orange solid. All materials were insoluble in common solvents but hot DMF and DMSO.

Table S1. Thermal behaviour of doped PUxH and PUxF samples

Sample	1st heating		2nd heating	2nd heating	T_d (°C)	inorganic wt%
	T_m (°C)	T_m (°C)	T_m (°C)	T_g (°C)		
PU0H	145	164	132.8	—	457	0
PU1H	137	158	167.3	—	466	2
PU10H	123	147	148.8	—	394	9
PU20H	131	152	156.2	—	432	14
PU50H	158.3	—	—	—	434	33
PU0F	—	—	—	-44.1	472	0
PU1F	—	—	—	-42.5	457	2
PU10F	—	—	—	-46.0	459	9
PU20F	—	—	—	-36.6	448	17
PU50F	—	—	—	—	442	43

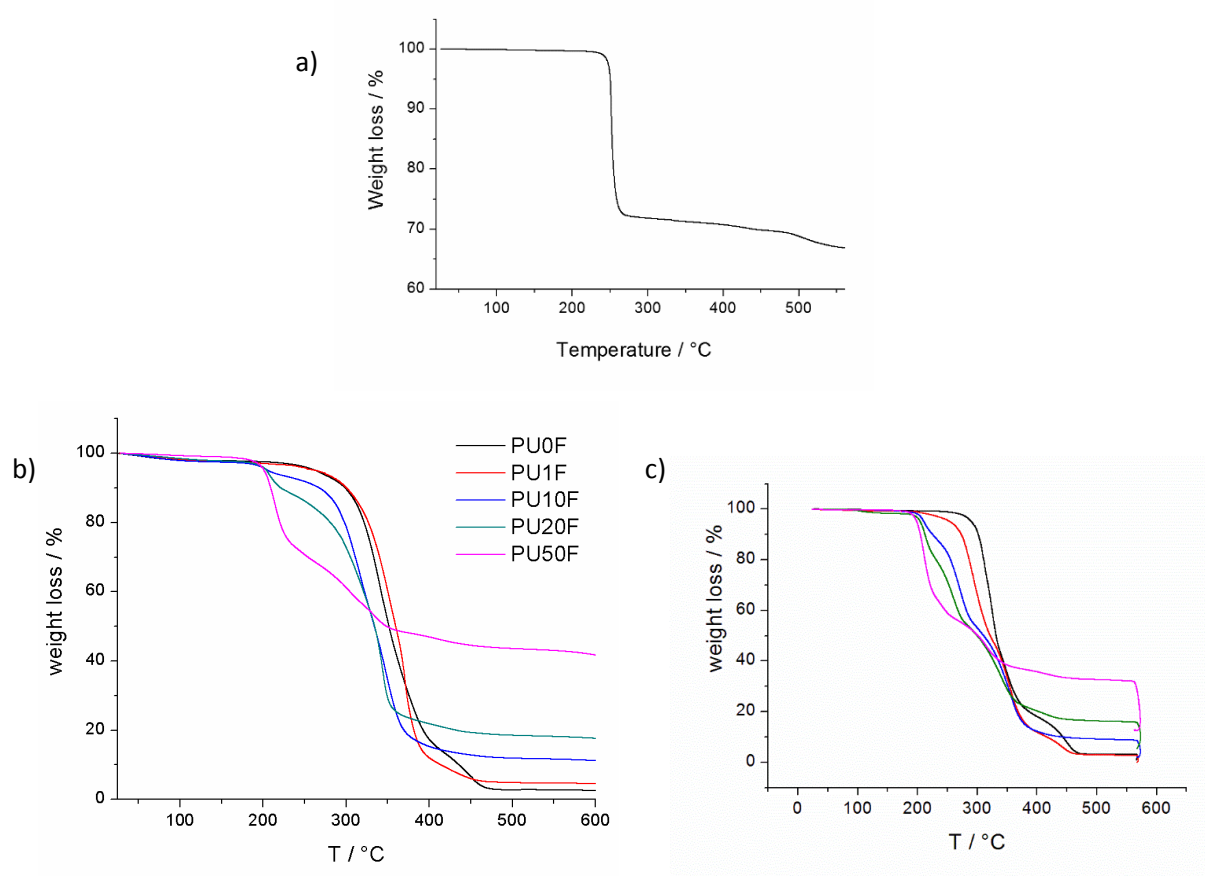


Fig. S1 TGA thermograms obtained at 10 K min⁻¹ heating rate for a) $Cs_2Mo_6I_8(OCOC_2F_5)_6$ b) PUxF samples and c) PUxH samples, black line: x = 0; red line: x = 1; blue line: x = 10; green line: x = 20; magenta line: x = 50.

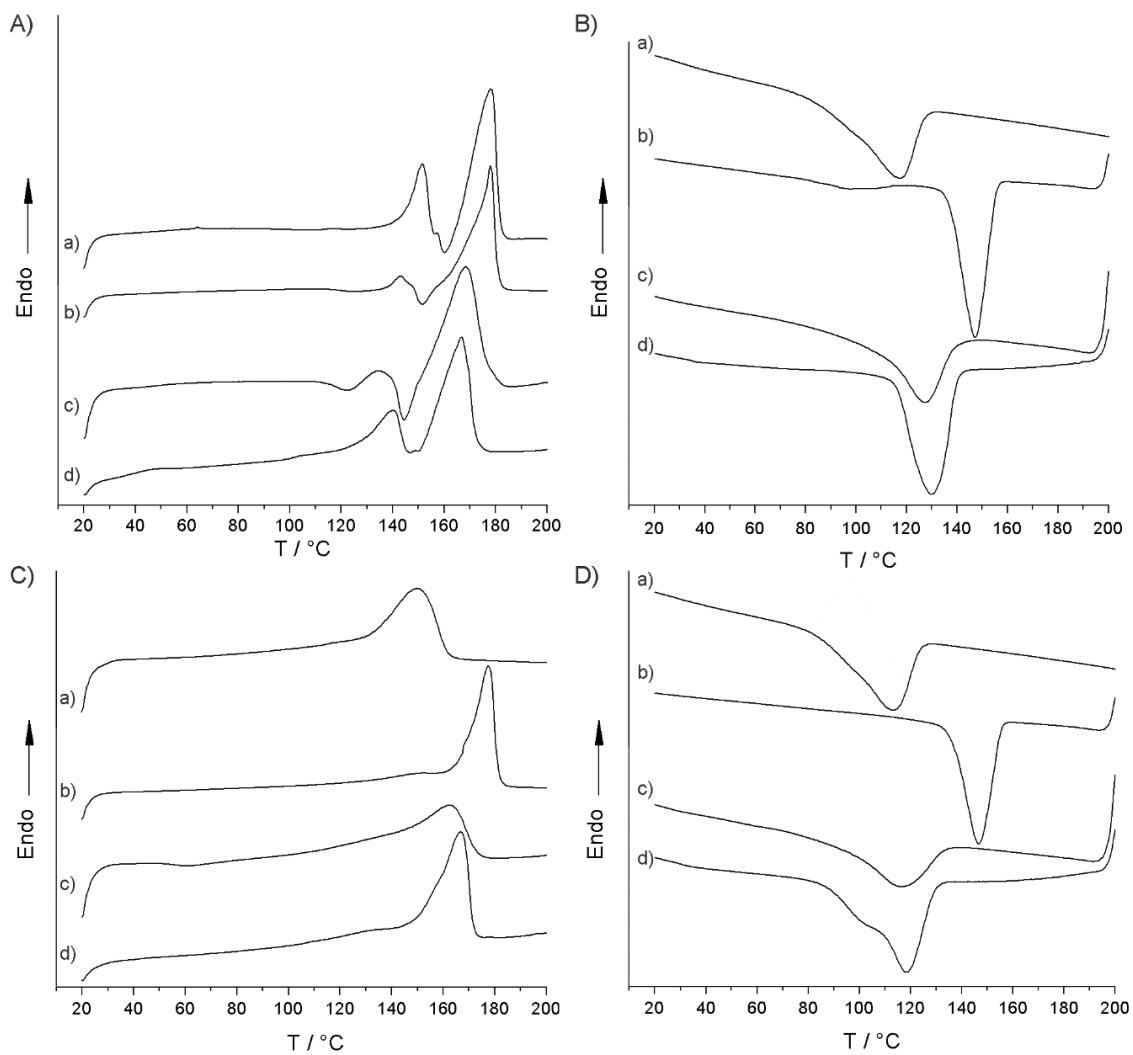


Fig. S2 DSC Thermograms of PU_xH samples with a) PU₀H, b) PU₁H, c) PU₁₀H and d) PU₂₀H; A: first heating, B) first cooling, C) second heating, D) second cooling.

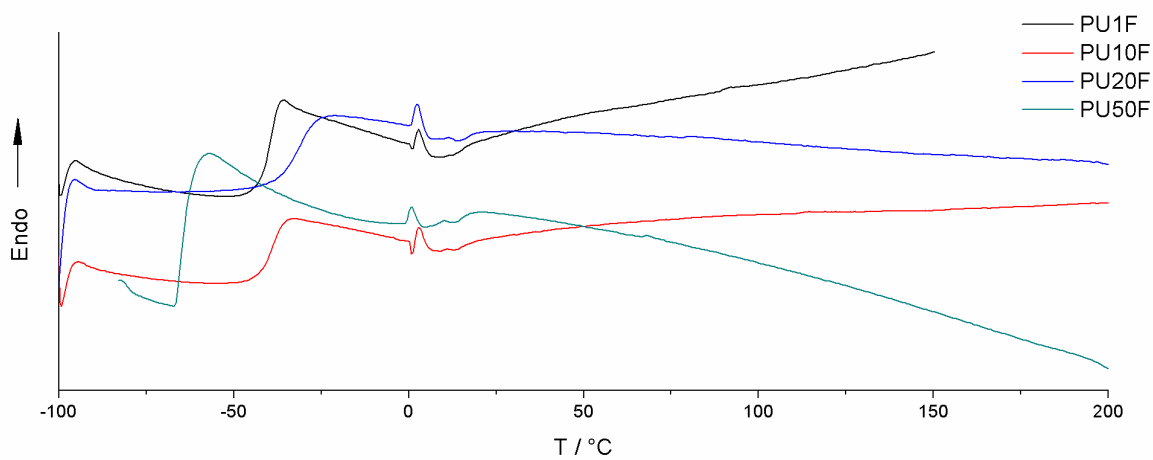


Fig. S3 DSC thermograms obtained on heating at 10 K min⁻¹ for PU_xF samples

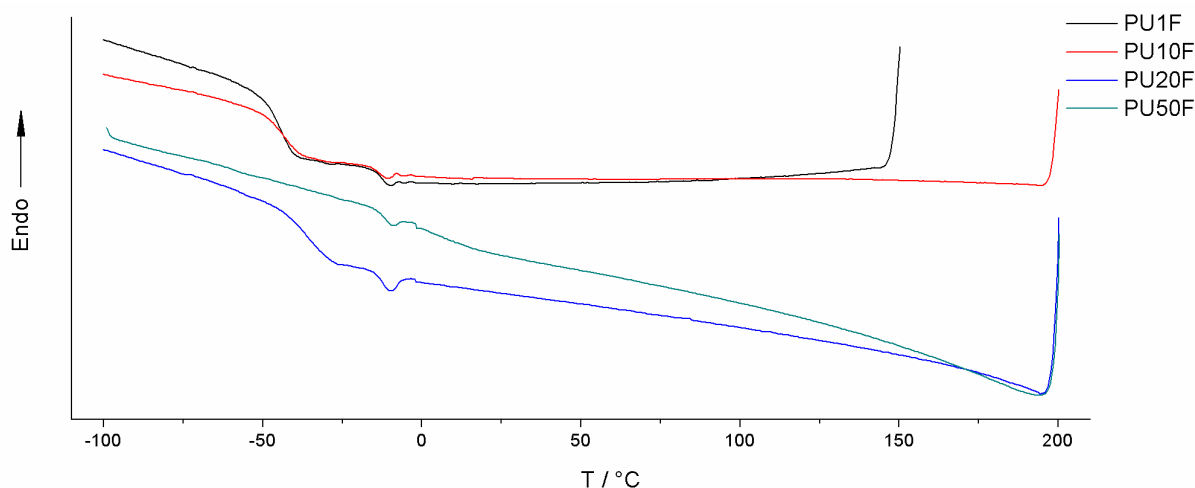


Fig. S4 DSC thermograms obtained on cooling at 10 K min^{-1} for PUxF samples

The DSC thermograms of the heating and cooling cycles of PUxH are depicted in fig S2, and the values of the first and second heating cycle are shown in table S1. In the first heating cycle, two melting endothermic transitions were observed for all PUxH samples but for PU50H (values) which can be assigned to different ordering inside the crystalline domains due to hydrogen bonding. This behaviour has been already described for other non-segmented polyurethane systems and it has to be noted that the appearance, the shape and size of these endothermic transitions strongly depend on the synthesis and annealing time and temperatures of the polymers. In the cooling cycle, there appears only one broad melting transition. In subsequent heating cycles, the highest melting endotherm transition, compared to the first heating, is stabilized for PU1H, PU10H and PU20H. Surprisingly, for PU without cluster, the melting transition stabilized was the lower one. For PU50H only one broad transition was observed in the first heating thermogram along with some decomposition occurring at $190 \text{ }^\circ\text{C}$. From the second heating thermogram an increase in the melting transition temperature was observed with the amount of cluster introduced. For PUxF samples: In the first heating a very broad peak (between 20 and $140 \text{ }^\circ\text{C}$, data not shown) was observed which can be attributed to the melting of the hard domains. This transition could not be detected in further cycles which may be due: i) to the more irregular structure obtained by the one step bulk polymerization compared to the two step, prepolymer method in which the soft prepolymer is formed in a first step and the hard domain is formed in a second step and ii) to the low percentage of hard segment in the PU hybrid which does not allow the formation of hard domains. As expected the T_g increased with the ratio cluster/PEG.

The degradation of PU is a multi-stage process whose complexity increases with the content of Mo_6 cluster units. For PU0F and PU1F containing 0 and 1 wt\% of cluster units respectively, the TGA curves showed only two step of weight loss one at $300 \text{ }^\circ\text{C}$ for both polymers and a second step starting at $400 \text{ }^\circ\text{C}$ for PU0F or $380 \text{ }^\circ\text{C}$ for PU1F. For PU10F, PU20F and PU50F, an additional step of weight loss appeared at $250 \text{ }^\circ\text{C}$ which was attributed to the loss of the six pentafluoropropionate ligands of the cluster unit. An additional step was observed for PU hybrids powders around $325 \text{ }^\circ\text{C}$ that is attributed to the degradation of hard domains. The TGA curves of PUxH for 0 and 1 wt\% of cluster units, showed three weight loss steps one at 330 and $320 \text{ }^\circ\text{C}$, respectively attributed to the decomposition of the hard domains. The second step of weight loss was observed for both at $380 \text{ }^\circ\text{C}$. For PUxH containing 10 , 20 and 50 wt\% of cluster units a first step of weight loss appeared at $250 \text{ }^\circ\text{C}$, which corresponds to the loose of the six pentafluoropropionate groups in apical position of the cluster core. The weight loss increased at this temperature as the amount of cluster units increased. A second step of weight loss for these three hybrids was observed at starting temperatures of 287 , 270 and $260 \text{ }^\circ\text{C}$, respectively which indicates that the addition of Mo_6 cluster unit destabilizes the hard segment microdomains.

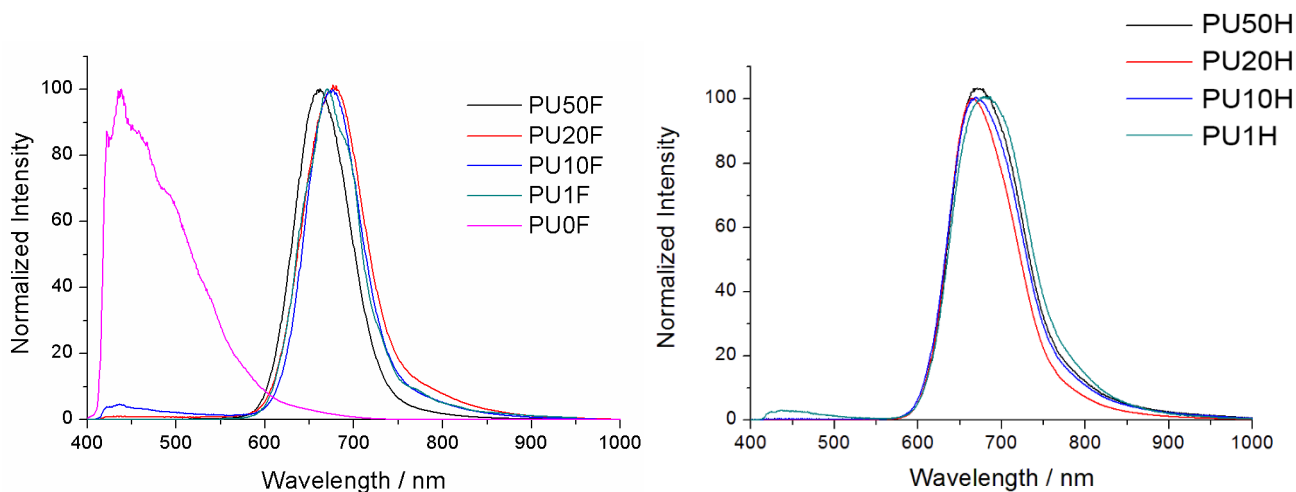


Fig. S5 Normalized luminescence spectra obtained for PUxF (left) and PUxH (right) samples under irradiation at 360 nm.

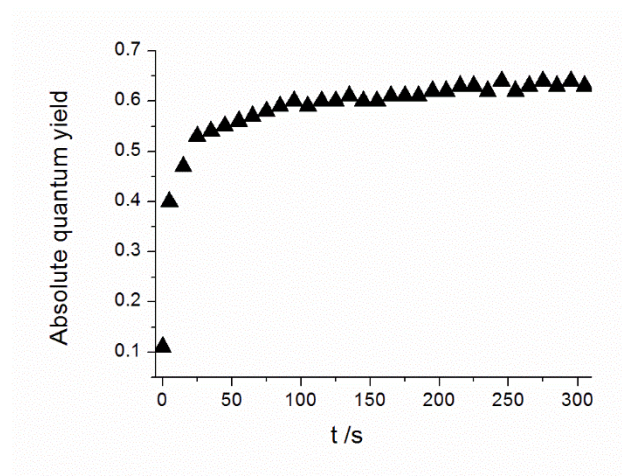


Fig. S6 Evolution of the absolute quantum yield of a PU50F sample placed within the integrating sphere upon constant N₂ gas flow (P= 0.4 mbar).

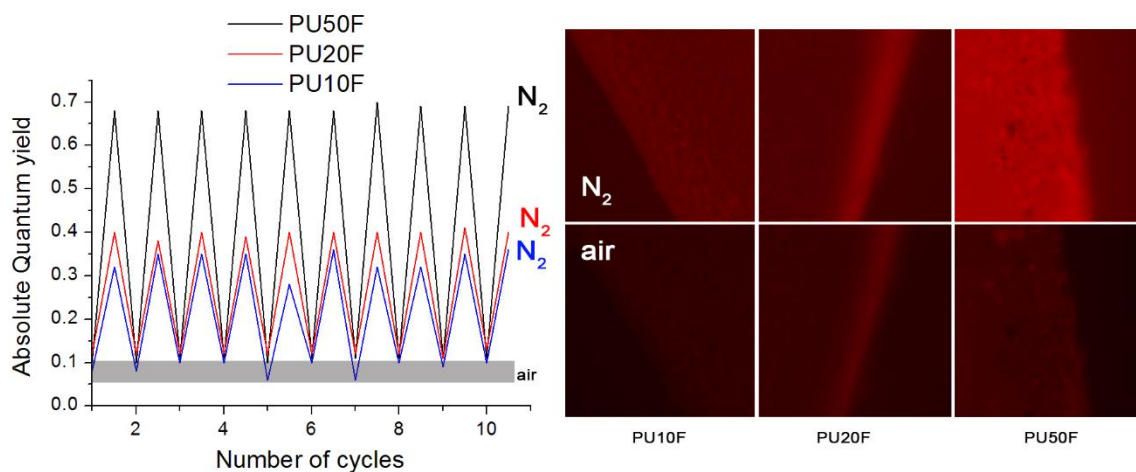


Fig. S7 Evolution of the quantum yield values upon air/N₂ atmosphere cycling, right: pictures taken under irradiation (integration time: 100ms) of PUxF samples

Table S2. Photophysical parameters of PUxF (x=n 1, 10, 50) under air and N2 gas stream

Samples	In air					in N ₂ stream				
	A ₁ (10 ⁻³)	τ ₁ (μs)	A ₂ (10 ⁻³)	τ ₂ (μs)	R ²	A ₁ (10 ⁻³)	τ ₁ (μs)	A ₂ (10 ⁻³)	τ ₂ (μs)	R ²
PU1F	0.33	6.9	0.73	60.2	0.9972	0.27	6.6	0.86	88.2	0.9966
PU10F	0.53	13.4	2.04	70.0	0.9996	0.27	7.3	3.17	95.8	0.9995
PU50F	4.71	10.9	4.28	33	1	3.58	9.5	8.64	56.1	0.9999

$$I(t) = I_0 + A_1 \exp(-t/\tau_1) + A_2 \exp(-t/\tau_2)$$

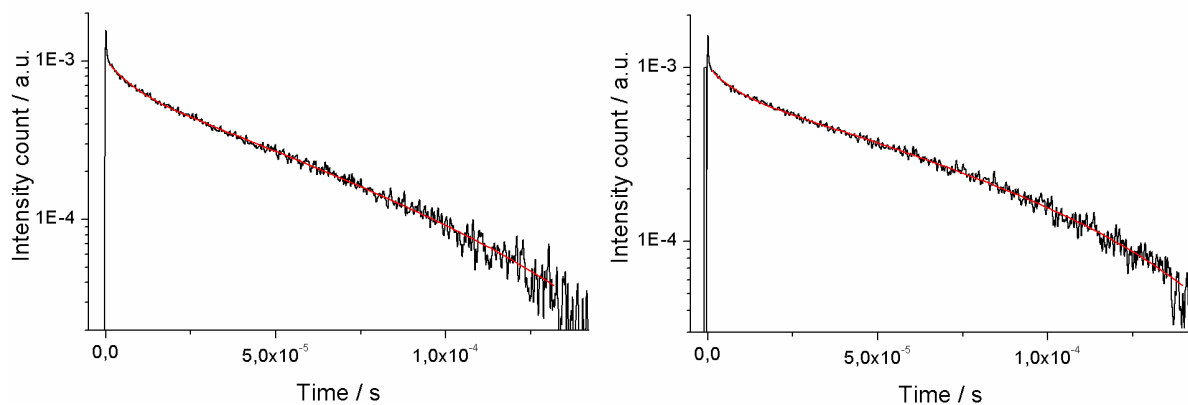


Figure S8 Phosphorescence decay profiles (in black) and calculated fit (in red) for PU1F in air (left) and with a N₂ stream (right)

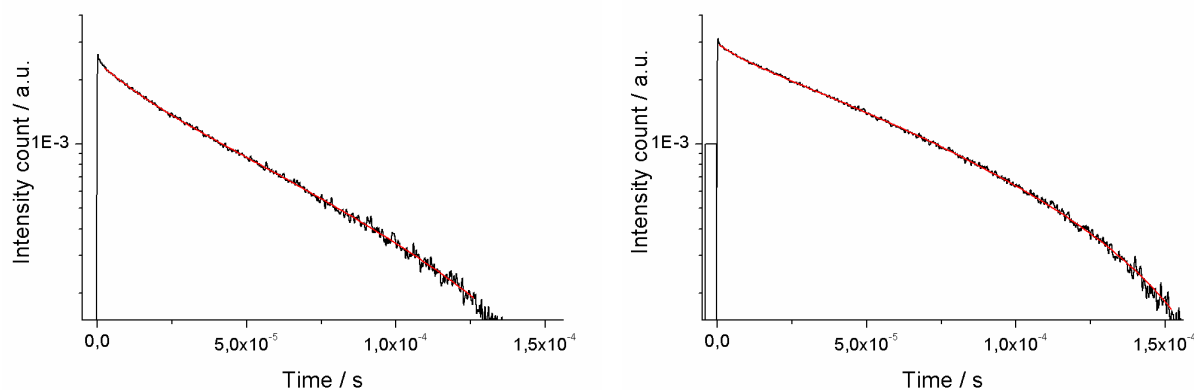


Figure S9 Phosphorescence decay profiles (in black) and calculated fit (in red) for PU10F in air (left) and with a N₂ stream (right)

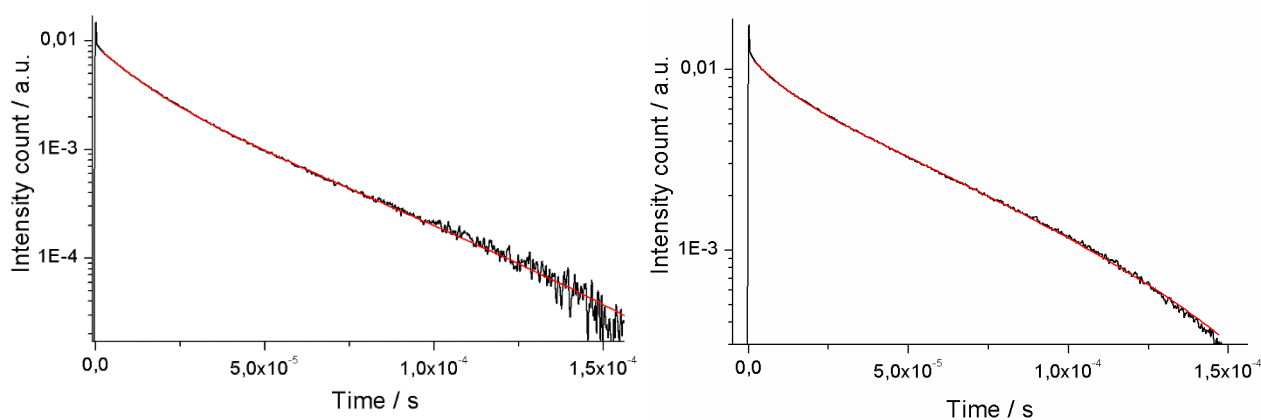


Figure S10 Phosphorescence decay profiles (in black) and calculated fit (in red) for PU50F in air (left) and with a N₂ stream (right)